JOURNAL OF MATERIALS SCIENCE 26 (1991) 3486–3490

Role for plastic flow in ambient-temperature cracking behaviour at hardness indentations in silicon crystals

HYUNGJAE SHIN, R. W. ARMSTRONG
University of Maryland, College Park, MD 20742, USA
I. L. SINGER
Naval Research Laboratory, Washington, DC 20375, USA

New indentation hardness measurements on silicon crystals are correlated with previous results obtained over a wide range of load values to analyse the ambient-temperature cracking behaviour. From an elastic–plastic–cracking analysis of the total results, brittle cracking is reasoned to be promoted by any amount of plastic deformation occurring during the initial indenting process.

1. Introduction

Frank and Lawn [1] and, then, Lawn [2], with coworkers [3–5], have developed the method of indentation fracture mechanics to gauge the brittleness of ceramics and related materials. The indentation fracture mechanics analysis was employed to explain Auerbach's law that the ratio of load to ball (indenter) radius is constant for the onset of cone cracking. Since then a whole variety of indenter shapes and crack geometries have been analysed on a similar basis. For a fixed indenter shape, a fully developed crack length proportional to the 2/3 power of load is generally obtained.

In the various descriptions of these cracking experiments [6], little use is made of the plastic indentation sizes or the hardness values determined by them. In particular the concern here is whether cracking is preceded by plastic flow even in the most brittle material, and to what extent the pre-crack plastic deformation influences the occurrence of cracking. Also, there is the question of the extent to which eventual cracking lowers the plastic hardness.

MgO crystals have been shown to exhibit {1 1 0} cracking at Vickers indentations that was explained in detail on a deformation-induced dislocation reaction basis [7]. A comparison has been made recently of the reduced hardness of MgO crystals caused by such cracking relative to deformation-induced cracking in essentially brittle crystals of cyclotrimethylenetrinitramine, $(CH_2 \cdot N \cdot NO_2)_3$, crystals where the hardness was only slightly reduced as a greater extent of cracking occurred [8]. Additional scanning electron microscope observations of Vickers indentations on an MgO crystal have been assessed in terms of elastic and plastic deformations accompanying the indentation process [9]. A Hertzian analysis of hardness stresses and strains was employed to interpret the results. In the present report, attention is focused on silicon as studied in the early work by Lawn [2] and for which results have now been obtained over a wide range of conditions [10–13].

2. Previous and current experiments

Previous indentation results on silicon crystals are described in this section along with current results obtained here. Relevant measurements for the analysis given in this investigation are listed in Tables I and II.

2.1. Results with sharp indenters

Pethica *et al.* [10] tested single-crystal silicon at very low loads with a special depth-sensing microhardness tester (see Table I). The diamond Berkovitch pyramid, which has a triangular base with a nominal angle of 65.3° between the face and vertical axis, was used as an indenter. Indents were produced without causing fracture for loads less than 0.05 N. Particular data reported at two load values and, also, a lowest indentation measurement shown graphically by Pethica *et al.* are used in Fig. 1 to define a range of silicon crystal indentations in an elastic–plastic regime. Near to the lowest load value is shown a computed Hertzian elastic curve (to be described) on the basis of taking the test with a Berkovitch indenter to be equivalent to performing a ball indentation test with a ratio of the circular indentation diameter to ball diameter, d/D, equal to 0.418. The d/D ratio is calculated in the same manner as $d/D = 0.375$ is taken as the ball indentation equivalent of a Vickers indentation [14]. The equivalent ball diameter according to this method is taken to give an indentation tangent to the indenter facets at the surface traces of the residual triangular indentation. For convenient comparison with the other Vickers data in Fig. 1, the computed D values for the Berkovitch indentations have been employed to determine equivalent d_i values for the Vickers indentations using $d = 0.375D$ and $d_i = 2^{1/2}d$.

0022–2461/91 $03.00 + .12

TABLE I Indentation test data with sharp indenter for silicon single crystals[a]

Investigators	Indenter type	H_v (GPa)	P (N)	d_i (μm)	h^b (μm)	d_c (μm)
Pethica *et al.* [10]	Berkovitch	**28.0**	0.00015	(0.10)	**0.03**	**0.0**
		21.0	0.0017	(0.40)	**0.1**	**0.0**
		18.0	0.014	(1.25)	**0.3**	**0.0**
Chiang *et al.* [11, 12]	Vickers	**9.0**	**0.03**[c]	2.49	(0.3557)	**1.3**
Lankford and Davidson [13]	Vickers	**10.0**	**0.05**[c]	3.01	(0.4300)	**1.3**
Shin *et al.* (this work)	Vickers	11.34	1.03	13.01	(1.858)	36.73

[a] The values in bold characters were given by the investigators, while those in brackets were calculated with the assumption of perfect indenter shape.
[b] Depth of penetration.
[c] Load at crack initiation.

TABLE II Indentation test data with spherical indenter for silicon single crystals

Investigator(s)	Indenter type	D (mm)	P (N)	d_c[a] (mm)
Lawn [2]	Sintered WC	3.175	**70.06**	0.1720
		6.35	**127.7**	0.2647
		9.525	**219.5**	0.3630
		12.7	**279.0**	0.4327
		16.0	**353.0**	0.5055
Shin *et al.* (this work)	Stainless steel	1.5875	148.0	0.2830
		6.35	269.7	0.4381

[a] The diameter of the initial ring crack; calculated from other given values in Lawn's case, and measured under the microscope in our case.

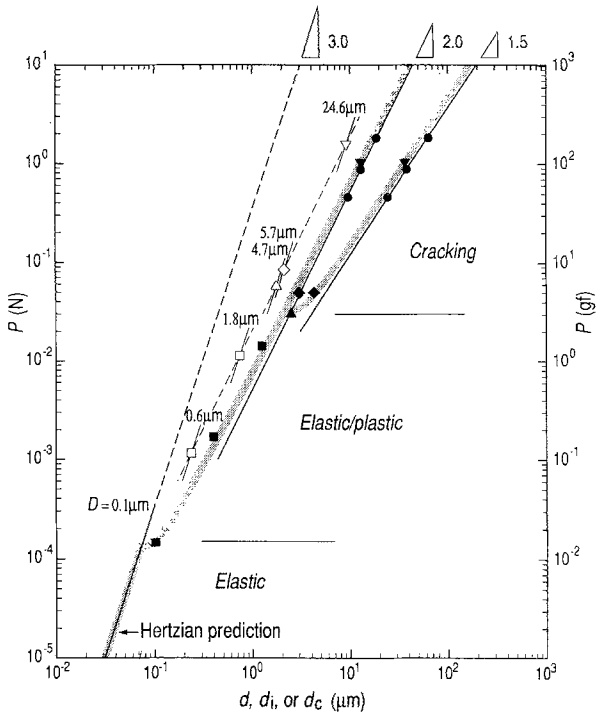

Figure 1 Variation of load, P, with diagonal lengths of contact area, d, indentation, d_i and radial crack, d_c, in logarithmic scale for indentations on silicon materials with sharp indenters. (●) This work, polycrystal; (▼) this work, single crystal; (◆) Langford and Davidson [13]; (▲) Chiang *et al.* [11, 12]; (■) Pethica *et al.* [10].

Chiang *et al.* [11, 12] and Lankford and Davidson [13] have provided valuable information for establishing the crack-initiation threshold with a Vickers indenter on silicon crystals at 0.03 and 0.05 N, respectively, as shown also in Fig. 1. For Lankford and Davidson's study, as-grown surfaces of crystals were subjected to loads over a range from ~0.01 to 60 N. These investigators and others [4, 5] have employed both plastic indentation and crack size measurements to gauge the brittleness of silicon and other ceramic materials.

For this part of the present study, we have tested polycrystal and single-crystal silicon materials with a Tukon microhardness tester. Three polycrystal specimens were tested with three different loads (~0.5, 0.9, and 2.0 N) using a Vickers diamond pyramid indenter. Ten indentations were made at each load on each specimen. The polycrystal results were employed for general estimation of the hardness and the cracking behaviours that are shown in Fig. 1. Three single-crystal specimens with a {0 0 1} surface orientation were tested also at the single load value of 1.03 N and with 20 indentations for each specimen.

2.2. Results with spherical indenters

Lawn [2] performed a pioneering series of tests on lightly abraded {1 1 1} surfaces of silicon single crystals with five different sizes of sintered tungsten carbide ball indenters ranging from 3.175 to 16 mm in diameter. Those results are shown in Fig. 2. Several continuously loaded indentations were performed here on well polished {1 1 1} silicon specimens for comparison with the earlier work of Lawn which presaged the advent of indentation fracture mechanics. The current indentation tests were performed with 1.5875 and 6.35 mm diameter stainless steel balls in a thermal expansion-driven continuous indentation system that provided an autographic record of load and ball displacement [15]. As reported by Lawn, the Hertzian ring cracks occurred in a hexagonal shape because of cracking on {1 1 1} for the crystallographic orientation of the single-crystal specimen, as identified in Fig. 3.

3. Relationships between P and d, d_i, or d_c

The theoretical elastic curve for the load, P, dependence on the contact diameter, d, is derived from the

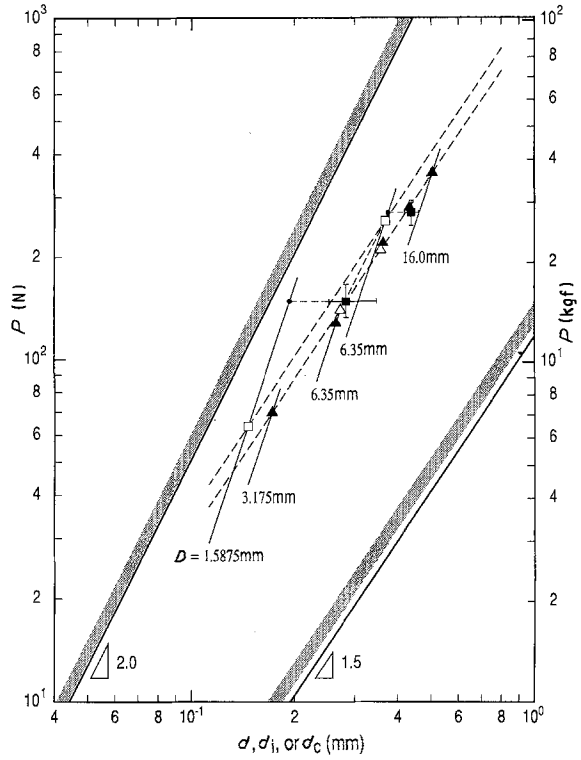

Figure 2 Variation of load, P, with diagonal lengths of contact area, d, indentation, d_i and radial crack, d_c, in logarithmic scale for indentations on silicon single crystals with spherical indenters. (▲) Lawn [2], abraded {1 1 1} crystal; (■) this work, unabraded {1 1 1} crystal.

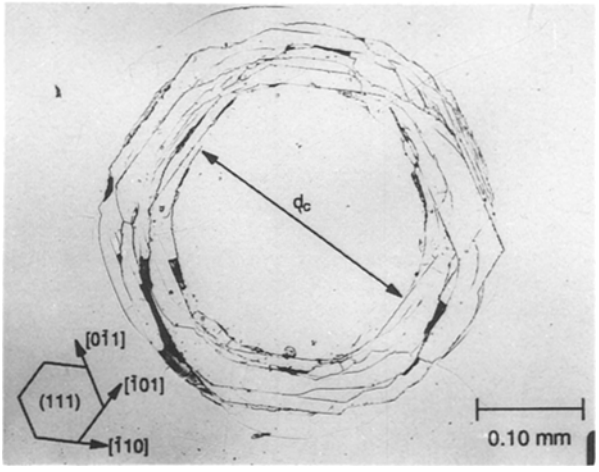

Figure 3 Multiple ring cracks produced with 1.5875 mm ball indenter on (1 1 1) surface. Identified crystallographic directions of crack traces and the initial ring crack diameter are indicated.

classical description of Hertz as

$$P = \frac{1}{3D}\left(\frac{1-\nu_b^2}{E_b} + \frac{1-\nu_s^2}{E_s}\right)^{-1} d^3 \qquad (1)$$

where D is the ball diameter and E_b, E_s, ν_b and ν_s are the elastic moduli and the Poisson's ratios for the indenter and the specimen, respectively. The elastic modulus and Poisson's ratio used for silicon are 1.627×10^5 MPa and 0.223; for indenters they are 2.04×10^5 MPa and 0.28, 5.34×10^5 MPa and 0.22, and 1.05×10^6 MPa and 0.2 for stainless steel, tungsten carbide and diamond, respectively. For $D = 0.1$ μm, the line of slope 3.0 shown in Fig. 1 is obtained.

The conventional Vickers hardness, H_v, equation can be rewritten in terms of P and the residual indentation diagonal, d_i, as

$$P = \left(\frac{H_v}{1.8544}\right) d_i^2 \qquad (2)$$

Finally, the relationship between P and the diagonal crack length, d_c, is obtained from the residual stress intensity, K_r, equation reported as [4]

$$P = \left(\frac{K_r}{2^{1.5}\chi_r}\right) d_c^{1.5} \qquad (3)$$

with the constant $\chi_r = \S_r^R(\cot\psi)^{2/3}(E_s/H)^{1/2}$, where H is the Meyer hardness, $\S_r^R$ is an experimental dimensionless term independent of the indenter/specimen system and taken as 0.032 ± 0.002, and ψ is the angle between the vertical axis and the indenter diagonal edge which is 74° for a Vickers indenter.

4. Results and discussion

The total data analysed in the present investigation were placed on logarithmic plots of P against d, d_i, or d_c in order to study the relationship between plastic flow and cracking, as shown in Figs 1 and 2. Fig. 1 is constructed with lines for the three different slopes: 3 for elastic loading; 2 for plastic loading (or hardness); and 1.5 for cracking on an indentation fracture mechanics basis. In addition to the elastic loading line for a 0.1 μm diameter ball corresponding to the smallest load datum of Pethica *et al.* [10], the hardness and cracking lines are drafted from our polycrystalline results that line up very well with the results of these previous investigators.

Beginning from the results at lowest loads with a sharp indenter, the low-load, elastic–plastic part of the graph is established so as to indicate a transitional stage between the elastic loading line and the plastic loading line. Following on at larger loads, the data of Chiang *et al.* [11, 12] and Lankford and Davidson [13] mark reasonably closely the initiation of cracking. Our experiments give results located in the region of well-developed cracking where the predictions from Equations 2 and 3 are clearly demonstrated. A set of broad shaded lines is drawn to illustrate the trends of these data.

A number of equivalent elastic indentation results are shown in Fig. 1 to contrast with the actual hardness data. Besides the main elastic loading line, other short lines with a slope of 3 were drawn for the various points in accordance with Equation 1, also obtaining a D value in each case from the relationships $d = d_i/2^{1/2}$ and $D = d/0.375$. The open symbol points were placed at their respective d values on each elastic loading line segment, thus giving an equivalent elastic hardness value at the pre-determined d/D ratio. The resultant two sets of open points are connected by slightly displaced but otherwise parallel dashed lines representing the hardness relationship for equivalent elastic indentations corresponding to the (lower) Berkovitch

results and the (upper) Vickers ones. Although all of the actual hardness measurements with the Berkovitch indenter are shown in Fig. 1 as converted to Vickers measurements, the equivalent elastic indentation values have been computed for the larger Berkovitch d/D ratio of 0.418.

On an equivalent elastic indentation basis, one can observe that d for pure elastic loading is increased to d_i when plastic flow occurs and the hardness is lowered. A further increase in d_i occurs when cracking is initiated and the "elastic load" required to satisfy the d/D ratio being constant changes over from being less than the actual load to more than that load. As a result, the hardness is lowered further. The hardness measurements for cracked indentations that have plastically flowed are less than the values elastically predicted.

In the case of spherical indentations, Lawn's series of indentations show very good agreement in Fig. 2 with estimations from Auerbach's law over a range of indenter sizes: $3.175\,\text{mm} \leq D \leq 16\,\text{mm}$. The open symbols here are for Lawn's assumption of a constant ratio of load to indenter radius. His measurements were made after scratches of $\sim 10\,\mu\text{m}$ in depth were introduced by abrading the (1 1 1) crystal surface with 600 SiC paper. For these conditions, Lawn [2] estimates that the "law" should be obeyed over a range of ball diameters between 1.0 and 100 mm. All of these measurements occurred at a lower hardness pressure than the plastic hardness value obtained if the crack diameter is taken equal to the residual indentation diameter. However, the measurements fit within a significantly lower ratio of $0.0316 \leq d/D \leq 0.0542$ that should give plastic hardness values less than the Vickers plastic hardness line, according to the extent to which the hardness is reduced at smaller plastic strains [9]. On the other hand, Wilshaw [16] has called attention to the experimental observation that crack diameters even larger by a factor of two times the actual contact diameters have been reported for glass materials, and explained on the basis of varying crack size distributions around the indenter contact areas. The presumption adopted here, though, is that Lawn's abraded surface measurements have given a contact area essentially equal to the area enclosed by ring cracking. In this regard, the dashed line of slope 1.5 through Lawn's experimental data may be extrapolated to intersect the elastic cracking points computed at D values of 4.7 and 5.7 μm in Fig. 1, thus indicating from consistency with these other measurements that Lawn's cracking diameters are at least close to the actual contact diameters.

The new cracking points measured here on an unabraded surface, for example at $D = 6.35$ mm, are in an even lower hardness region, however, than the results reported by Lawn, and this creates a problem of understanding how the hardness stress for cracking should be greater if abrading the crystal has only enhanced the distribution of crack embryos for the elastic Hertzian fractures. This gives substance to the proposal that there is at least a small plastic strain contribution to the cracking measurements made here. The open square results in Fig. 2 relate to this issue. They are computed on the reasonable theoretical basis that the elastic hardness of Lawn's material and of the material used here are the same (see the dashed line of slope 2.0 connecting the computed result for Lawn at $D = 6.35$ mm to the intersection point with the new Hertzian elastic curve reported here at the same D value). The computed (open square) elastic hardness value corresponding to the 6.35 mm ball is shown to be greater than the actual hardness measurement. An analogous result is shown for the comparison at $D = 1.5875$ mm, except that the difference between the computed and measured results is even greater. The dashed line for the theoretical "elastic load" values at cracking for the new measurements clearly shows a greater role for plastic deformation in initiating cracking at the ball size of 1.5875 mm as compared with the result for $D = 6.35$ mm. The result connects very directly with the practical observation that plastic deformation is more likely to be observed as the indenter ball diameter is smaller. In both cases the elastic hardness values obtained by extrapolating the Hertzian curves to the same loads as employed in making the measurements give even larger hardness values compared to the measurements (see the dashed horizontal lines at the P values of 148 and 270 N). As a final point relating to Fig. 3, the occurrence of successive stages in interconnected plastic flow and cracking processes is a possible explanation of the observed result that a number of separated irregular crack initiations are observed, in some cases also connecting with naturally occurring surface scratches.

5. Summary

An elastic–plastic–cracking method of analysis applied to previous and new indentation test results on silicon crystals indicates that plastic flow initiated in the indentation process, even for this brittle material at ambient temperature, contributes to easier cracking than should occur for totally elastic behaviour. The method of analysis appears to be useful for establishing the relationship between hardness and cracking measurements made with sharp or spherical indenters.

Acknowledgement

This research activity has been supported in part by the Office of Naval Research under Contract N00014-86-0286, NR 432h-021, and represents a portion of the PhD thesis research of H.S.

References

1. F. C. FRANK and B. R. LAWN, *Proc. R. Soc.* **A 299** (1967) 291.
2. B. R. LAWN, *J. Appl. Phys.* **39** (1968) 4828.
3. B. R. LAWN and E. R. FULLER, *J. Mater. Sci.* **19** (1984) 4061.
4. B. R. LAWN, A. G. EVANS and D. B. MARSHALL, *J. Amer. Ceram. Soc.* **63** (1980) 574.
5. G. R. ANTIS, P. CHANTIKUL, B. R. LAWN and D. B. MARSHALL, *ibid.* **64** (1981) 533.
6. C. B. PONTON and R. D. RAWLINGS, *Mater. Sci. Technol.* **5** (1989) 865.

7. R. W. ARMSTRONG and C. Cm. WU, *J. Amer. Ceram. Soc.* **61** (1978) 102.
8. R. W. ARMSTRONG and W. L. ELBAN, *Mater. Sci. Engng* **A 111** (1989) 35.
9. B. L. HAMMOND and R. W. ARMSTRONG, *Phil. Mag. Lett.* **57** (1988) 41.
10. J. B. PETHICA, R. HUTCHINGS and W. C. OLIVER, *Phil. Mag. A.* **48** (1983) 593.
11. S. S. CHIANG, D. B. MARSHALL and A. G. EVANS, *J. Appl. Phys.* **53** (1982) 298.
12. *Idem, ibid.* **53** (1982) 312.
13. J. LANKFORD and D. DAVIDSON, *J. Mater. Sci.* **14** (1979) 1662.
14. D. TABOR, "The Hardness of Metals" (Clarendon, Oxford, 1951) p. 98.
15. J. J. LESKO and R. W. ARMSTRONG, Application to US Patent and Trademark Office, February 1990, File No. 2284-023-6.
16. T. R. WILSHAW, *J. Phys. D* **4** (1971) 1567.

Received 13 August 1990
and accepted 25 January 1991